Anal. Chem. **2007,** *79,* 8136−8143

Microcantilever-Based Sensors: Effect of Morphology, Adhesion, and Cleanliness of the Sensing Surface on Surface Stress

Vincent Tabard-Cossa,[†,‡] Michel Godin,[†,§] Ian J. Burgess,[∥,⊥] Tanya Monga,[†,∥] R. Bruce Lennox,*[,∥] and Peter Grütter*[,†]

Department of Physics and Department of Chemistry, McGill University, Montréal, Québec, Canada

The surface stress response of micromechanical cantilever-based sensors was studied as a function of the morphology, adhesion, and cleanliness of the gold sensing surface. Two model systems were investigated: the adsorption of alkanethiol self-assembled monolayers at the gas−solid interface and the potential-controlled adsorption of anions at the liquid−solid interface. The potential-induced surface stress, on a smooth and continuous polycrystalline Au(111)-textured microcantilever in 0.1 M $HClO_4$, is in excellent agreement with macroscopic Au(111) single-crystal electrode results. It is shown that ambient contaminants on the sensing surface dramatically alter the surface stress-potential response. This observation can be misinterpreted as evidence that for polycrystalline Au(111) microcantilever electrodes, surface stress is dominated by surface energy change. Results for anions adsorption on gold are in contrast to the gas-phase model system. We demonstrate that the average grain size of the gold sensing surface strongly influences the magnitude of the surface stress change induced by the adsorption of octanethiol. A 25-fold amplification of the change in surface stress is observed on increasing the average gold grain size of the sensing surface from 90 to 500 nm.

The advent of atomic force microscopy (AFM) and advances in microelectromechanical systems (MEMS) have allowed microcantilevers to emerge as a promising new class of biochemical sensors. Chemical/physical reactions occurring on the microcantilever surface are detected as mechanical property changes of the cantilever beam. In one measurement mode, nanomechanical deflections of the cantilever are used to precisely detect changes in surface stress.[1] Surface stress measurements are at the basis of many intriguing sensing applications such as DNA,[2,3] RNA,[4] and protein[5,6] detection and analysis. However, in order for microcantilever-based surface stress sensing to become a viable technology, a better understanding of the parameters which determine the nature (compressive/tensile) and magnitude of the biochemically activated surface stress must be developed. We report here studies regarding the effect of the sensing surface on the induced surface stress by studying two model systems, the vapor phase alkanethiol adsorption on gold and the potential-controlled adsorption of anions on gold.

A very attractive feature of studying surfaces in an electrochemical environment is that the adsorption can be controlled by varying the electrode potential.[7] The development of microcantilever sensors to precisely measure surface stress changes at the solid−liquid interface in the late 1990s[8−14] revived interest in surface stress and surface energy[15] measurements. The resulting series of publications helped clarify the current knowledge of the thermodynamics of solid electrodes.[16−19] It is only recently[20] that

* Corresponding authors. Phone: +1 514 398 3638. E-mail: bruce.lennox@mcgill.ca (R. Bruce Lennox). Phone: +1 514 398 2567. E-mail: grutter@physics.mcgill.ca (Peter Grütter).

† Department of Physics, McGill University.

‡ Present address: Department of Physics & Astronomy, University of British Columbia, Vancouver, BC, Canada.

§ Present address: Massachusetts Institute of Technology, Biological Engineering Department, Cambridge, MA.

∥ Department of Chemistry, McGill University.

⊥ Present address: Department of Chemistry, University of Saskatchewan, Saskatoon, SK Canada.

(1) Berger, R.; Delamarche, E.; Lang, H. P.; Gerber, Ch.; Gimzewski, J. K.; Meyer, E.; Guntherodt, H.-J. *Science* **1997**, *276*, 2021.

(2) Fritz, J.; Baller, M. K.; Lang, H. P.; Rothuizen, H.; Vettiger, P.; Meyer, E.; Guntherodt, H.-J.; Gerber, Ch.; Gimzewski, J. K. *Science* **2000**, *288*, 316−318.

(3) McKendry, R.; Zhang, J.; Arntz, Y.; Strunz, T.; Hegner, M.; Lang, H. P.; Baller, M. K.; Certa, U.; Meyer, E.; Guntherodt, H.-J.; Gerber, Ch. *Proc. Natl. Acad. Sci. U.S.A.* **2002**, *99*, 9783−9788.

(4) Zhang, J.; Lang, H. P.; Huber, F.; Bietsch, A.; Grange, W.; Certa, U.; McKendry, R.; Güntherodt, H.-J.; Hegner, M.; Gerber, Ch. *Nat. Nanotechnol.* **2006**, *1*, 214−220.

(5) Wu, G.; Datar, R. H.; Hansen, K. M.; Thundat, T.; Cote, R. J.; Majumdar, A. *Nat. Biotechnol.* **2001**, *19*, 856−860.

(6) Savran, C. A.; Knudsen, S. M.; Ellington, A. D.; Manalis, S. R. *Anal. Chem.* **2004**, 76, 3194−3198.

(7) Bard A. J.; Faulkner L. R. *Electrochemical Methods*, 2nd ed.; Wiley: New York, 2001.

(8) Brunt, T. A.; Rayment, T.; O'Shea, S. J.; Welland, M. E. *Langmuir* **1996**, *12*, 5942−5946.

(9) Brunt, T. A.; Chabala, E. D.; Rayment, T.; O'Shea, S. J.; Welland, M. E. *J. Chem. Soc., Faraday Trans.* **1996**, *92*, 3807.

(10) O'Shea, S. J.; Welland, M. E.; Brunt, T. A.; Ramadan, A. R.; Rayment, T. *J. Vac. Sci. Technol., B* **1996**, *14*, 1383−1385.

(11) Raiteri, R.; Butt, H.-J. *J. Phys. Chem.* **1995**, *99*, 15728−15732.

(12) Miyatani, T.; Fujihira, M. *J. Appl. Phys.* **1997**, *81*, 7099−7115.

(13) Miyatani, T.; Fujihira, M. *Jpn. J. Appl. Phys.* **1997**, *36*, 5280−5281.

(14) Tian, F.; Pei, J. H.; Hedden, D. L.; Brown, G.M.; Thundat, T. *Ultramicroscopy* **2004**, *100*, 217. See also the published comments on this article by Lang, G. G.; Rokob, T. A; Horanyi, G. *Ultramicroscopy* **2005**, *104*, 330−332.

(15) Lang, G.; Heusler, K. E. *J. Electroanal. Chem.* **1994**, *377*, 1.

(16) Lipkowski, J.; Schmickler, W.; Kolb, D. M.; Parsons, R. *J. Electroanal. Chem.* **1998**, *452*, 193−197.

(17) Ibach, H. *Surf. Sci. Rep.* **1997**, *29*, 193−263.

(18) Schmickler, W.; Leiva, E. *J. Electroanal. Chem.* **1998**, *453*, 61−67.

10.1021/ac071243d CCC: $37.00
Published on Web 10/03/2007

some form of consensus on the subject has been reached in the electrochemical community (Lipkowski et al.,[16] Schmickler et al.,[18] and Guidelli[21]).

Unfortunately, many electrochemical microcantilever sensor results published to date are in contradiction to more recent surface stress results which have used other bending beam techniques.[16−18,22] In particular, surface stress results reported by Ibach et al.[23] and Haiss et al.[19] have a qualitatively different response at the solid−liquid interface than results employing microcantilever-based sensors. In these results,[24] obtained using an STM tip to measure the deflection of well-defined macroscopic Au(111) surfaces, the surface stress monotonically increased (i.e., no maximum) with increasing potential whereas a parabolic shape was observed using microcantilevers.[9−11] One notable difference between macroscopic electrodes and microcantilever electrodes is the ability to pretreat the surface of the former by flame-annealing to produce atomically flat single-crystal surfaces. On the other hand, the surface of a microcantilever-based sensor is made up of a polycrystalline evaporated thin film. This raises the possibility that the sensing surface morphology and its adhesion to the Si or SiN_x microcantilever beam influence the surface stress response and may explain the observed inconsistencies.[22] We have thus measured the potential-induced surface stress on an Au(111)-textured microcantilever to probe the origin of this discrepancy.

In an extensive literature review,[22] which tabulated various surface stress results obtained using microcantilever-based sensors, it was emphasized that there currently is little understanding and discussion on the origin of the surface stress generated by molecular adsorption. Notably, the parameters that affect the surface stress in a number of experiments remain unclear. We have thus measured the surface stress associated with the formation of alkanethiol self-assembled monolayers (SAM) from the vapor phase on Au(111)-textured microcantilevers as a model system for understanding the parameters influencing the observed change in surface stress. Specifically, we measured the surface stress generated by SAM formation as a function of the grain size of the gold sensing surface.

The role played by the state of the sensing surface in microcantilever sensors is often underappreciated though it can have a dramatic impact on the surface stress response as clearly demonstrated by Godin et al.[25] Previous studies[26−29] reported the effect of gold surface roughness and nanostructured interfaces on the microcantilever response for various analytes suggesting a correlation between surface stress and film roughness owing to a higher density of adsorption sites and an increase in intermolecular interaction within confined spaces. More recently Mertens et al.[30] showed that control of the gold coating process, forming either discontinuous or coalesced gold islands, is critical for the reliability of microcantilever sensors. These results indicate that parameters including adhesion (i.e., extent of transfer of the surface stress in the sensing film to the cantilever substrate), surface morphology (e.g., grain size, grain boundaries, film roughness, crystallographic orientation), and cleanliness (e.g., presence of contaminants on the sensing surface) of the gold sensing surface can have both qualitative and quantitative effects on the measured surface stress. It is therefore essential to characterize and prioritize how these affect the sensor response if microcantilever sensors are to become a useful technology.

EXPERIMENTAL SECTION

Instrumentation. Experiments performed at the solid−liquid interface involved an instrument constructed to integrate a microcantilever-based sensor with a standard three-electrode electrochemical system, the details of which are described elsewhere.[31] The electrochemical setup uses an Ag/AgCl reference electrode (model RE-6, BioAnalytical Systems, USA) and a platinum wire counter electrode (99.99% purity, Alpha Aesar, USA). Both are inserted into the top of a PTFE cell. A gold-coated, rectangular-shaped silicon microcantilever serves as both the working electrode (WE) and as the surface stress sensor. A potentiostat (model 50CW, BioAnalytical Systems, USA) was used to apply a potential to the microcantilever (WE) and to monitor the current response during cyclic voltammetric experiments. An optical beam technique[31,32] is used to simultaneously monitor the microcantilever deflection as a function of the applied electrochemical potential. The laser was focused on the silicon back side of the microcantilever to avoid artifacts in the deflection measurement which can result from changes in reflectivity of the gold-coated surface.[12]

To prevent electrochemical reactions at the contact point, the microcantilever (WE) was vertically immersed in the electrolyte with a micropositioner so that only the microcantilever and a small portion of the support chip (on which the cantilever beam is mounted) were exposed to the solution.

For the gas-phase experiments, as described previously,[32] the surface stress induced during SAM formation was measured in real time, using a custom-made microcantilever-based sensor, in a sealed aluminum cell, with a similar optical beam deflection technique.

Materials and Methods. All electrochemical experiments were performed in the cell described above. Prior to each experiment, the cell was rinsed three times with deionized water (Millipore Simplicity 185 water system), followed by the electrolyte solution. The 0.1 M perchloric acid ($HClO_4$) electrolyte solution

(19) Haiss, W.; Nichols, R. J.; Sass, J. K.; Charle, K. P. *J. Electroanal. Chem.* **1998**, *452*, 199−202.
(20) A publication, Marichev, V. A. *Surf. Sci. Rep.* **2005**, *56*, 277−324, continues to discuss certain thermodynamic problems of solid electrodes.
(21) Guidelli, R. *J. Electroanal. Chem.* **1998**, *453*, 69−77.
(22) Haiss, W. *Rep. Prog. Phys.* **2001**, *64*, 591−648.
(23) Ibach, H.; Bach, C. E.; Giesen, M.; Grossmann, A. *Surf. Sci.* **1997**, *375*, 107−119.
(24) These results by Ibach et al. and Haiss et al., on well-defined Au(111) surfaces using an STM tip to measure the deflection yielded good although not quantitative agreement with one another. Differences in the conversion of the cantilever deflection into a surface stress are most probably responsible for the differences in magnitude.
(25) Godin, M.; Williams, P. J.; Tabard-Cossa, V.; Laroche, O.; Beaulieu, L. Y.; Lennox, R. B.; Grütter, P. *Langmuir* **2004**, *20*, 7090−7096.
(26) Headrick, J. J.; Sepaniak, M. J.; Lavrik, N. V.; Datskos, P. G. *Ultramicroscopy* **2003**, *97*, 417−424.
(27) Lavrik, N. V.; Tipple, C. A.; Sepaniak, M. J.; Datskos, P. G. *Chem. Phys. Lett.* **2001**, *336*, 371−376.
(28) Hansen, A. G.; Mortensen, M. W.; Andersen, J. E. T.; Ulstrup, J.; Kuhle, A.; Garnæs, J.; Boisen, A. *Probe Microsc.* **2001**, *2*, 139−150.
(29) Desikan, R.; Lee, I.; Thundat, T. *Ultramicroscopy* **2006**, *106*, 795−799.
(30) Mertens, J.; Calleja, M.; Ramos, D.; Tarýn, A.; Tamayo, J. *J. Appl. Phys.* **2007**, *101*, 034904.
(31) Tabard-Cossa, V.; Godin, M.; Beaulieu, L. Y.; Grütter, P. *Sens. Actuators, B* **2005**, *107*, 233−241.
(32) Godin, M.; Laroche, O.; Tabard-Cossa, V.; Beaulieu, L. Y.; Williams, P. J.; Grütter, P. *Rev. Sci. Instrum.* **2003**, *74*, 4902−4907.

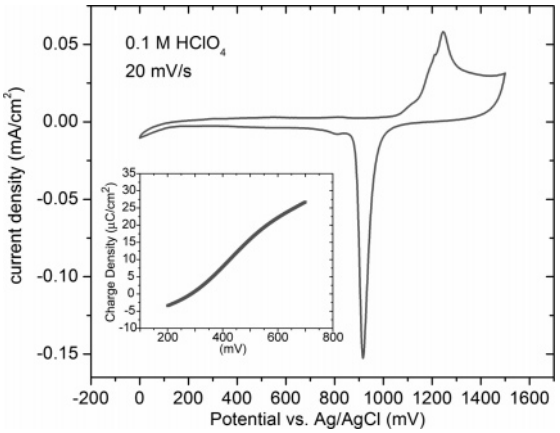

Figure 1. Cyclic voltammogram of the Au(111)-textured microcantilever in 0.1 M $HClO_4$. Scan rate of 20 mV/s. An SEM image of the gold surface is shown in Figure 3A. The gold oxide formed during the anodic sweep is stripped off by the cathodic sweep, as indicated by the presence of the sharp, cathodic peak at 930 mV. This process ensures that a fresh Au surface is exposed to the solution. The inset shows the surface charge density versus potential, within the electrical double layer region, determined by integration of the CV from +200 to +700 mV. A linear fit of the data gives a slope of 67 μF cm^{-2}.

was purged for 1 h with argon gas to remove oxygen contamination from the solution. A small positive pressure of argon is subsequently maintained above the electrochemical cell.

The microcantilever sensors used for the electrochemical experiments are rectangular Si cantilevers from MikroMasch (type CSC12/without Al/tipless) with a nominal length, width, thickness, and spring constant values of 350 μm, 35 μm, 1 μm, and 0.03 N/m, respectively. However, these exact dimensions and spring constant were independently measured by SEM for each microcantilever used in order to improve the accuracy of conversion of the cantilever deflection into a surface stress value.

A 100 nm film of Au (99.99%, Plasma Materials, USA) was deposited by thermal evaporation on one side of the silicon microcantilever onto a previously deposited 10 nm Ti (99.99%, Alfa Aesar, USA) adhesion layer. Evaporation was conducted at a pressure $< 5.0 \times 10^{-6}$ Torr at a rate of 0.14 nm/s for Au and 0.04 nm/s for Ti. Radiative heating of the evaporation boat increased the microcantilevers temperature to 130 ± 20 °C. The resulting Au film has an average grain diameter of 100 ± 60 nm with a rms roughness of 1.0 ± 0.2 nm, on a 1 μm length scale as determined by AFM. The surface stress measurements at the solid−liquid interface are performed on electrochemically cleaned gold surfaces. In some cases, Au films were produced via sputtering at various temperatures on a Nb (99.95%, Alfa Aesar, USA) adhesion layer.

By sweeping the voltage from 0 to +1500 mV as shown in Figure 1, the gold surface is cleaned via gold oxide formation and removal. The shape of the oxidation peak is related to the crystallographic texture of the gold film. A relatively sharp oxidation peak at 1220 mV indicates {111} textured gold.[33] This was corroborated with X-ray diffraction, which shows a predominance of a polycrystalline Au(111) texture.

For the gas-phase experiments, octanethiol ($HS(CH_2)_7CH_3$) was introduced into the second sealed cell described above by injection through a Teflon-lined septum. Liquid octanethiol (10−50 μL) was injected at a designated location in the closed cell. These experiments were conducted in the 3 mL cell with an octanethiol droplet-to-cantilever distance of 3 mm. The octanethiol then evaporated under ambient pressure and temperature in the presence of the gold coated microcantilever sensors.

To study the surface stress induced by the self-assembly of alkanethiol monolayers on Au(111)-coated microcantilevers, gold was thermally evaporated onto one surface of SiN_x microcantilevers, as described elsewhere.[26] The morphology of the resulting gold surfaces was highly dependent on the temperature during the evaporation. Au(111) surfaces exhibiting average grain diameters of 90 ± 50 nm up to 500 ± 400 nm were produced by varying the microcantilever temperature during evaporation from 30 °C to 280 °C.

Surface Stress and Thermodynamics of the Solid−Liquid Interface. The optical beam deflection technique used in these instruments accurately measures the deflection of the free end of a microcantilever, Δz.[34] The surface stress ($\Delta\sigma$) is in turn directly proportional to the microcantilever deflection (Δz) through a modified form of Stoney's equation:[34]

$$\Delta\sigma = \frac{4}{3(1-\upsilon)}\frac{l}{wt}k_{\mathrm{rect}}\Delta z \qquad (1)$$

where υ, l, w, t, and k_{rect} are the Poisson's ratio, length, width, thickness, and spring constant of the microcantilever, respectively. By carefully determining the value of each parameter in eq 1, one can measure surface stress values with an accuracy of 10% or better.[31,34]

The relationship between the surface stress, σ, and the surface free energy, γ, is described by the Shuttleworth equation:[35−37]

$$\sigma_{ij} = \gamma\delta_{ij} + \frac{\partial\gamma}{\partial\epsilon_{ij}} \qquad (2)$$

where ϵ_{ij} is the surface strain tensor and δ_{ij} is the Kronecker δ. In most cases of interest the surface stress tensor can take on a simple form. By an appropriate choice of the coordinate system, the off-diagonal components can be set to zero. Additionally, for surfaces possessing a 3-fold (e.g., the (111) surface of a face centered cubic, fcc, crystal) or higher symmetry (e.g., the 4-fold symmetry of the fcc (100) plane), the surface stress is isotropic and can assume a scalar form, σ.[38] By definition, a compressive (tensile) surface stress bends the microcantilever away from (toward) the stressed surface and is assigned a negative (positive) sign.

In order to understand the relative contribution of surface energy to the total measured surface stress we require the generalized Lippmann equation:

(33) Golan, Y.; Margulis, L.; Rubinstein, I. *Surf. Sci.* **1992**, *264*, 312−326.

(34) Godin, M.; Tabard-Cossa, V.; Williams, P. J.; Grütter, P. *Appl. Phys. Lett.* **2001**, *79*, 551−553.
(35) Shuttleworth, R. *Proc. Phys. Soc. London, Sect. A* **1950**, *63*, 444.
(36) Sanfeld, A.; Steinchen, A. *Surf. Sci.* **2000**, *463*, 157−173.
(37) Bottomley, D. J.; Ogino, T. *Phys. Rev. B* **2001**, *63*, 165412.
(38) Because $\sigma_{zz} = 0$ and $\sigma_{xx} = \sigma_{yy}$.

$$\left(\frac{\partial\gamma}{\partial E}\right)_{T,\mu_k} = -q + (\sigma_{ij} - \gamma\delta_{ij})\left(\frac{\partial\epsilon_{ij}}{\partial E}\right)_{T,\mu_k} \quad (3)$$

where q is the charge density on the electrode surface and E the electrode potential. For liquids, the second term on the right-hand side vanishes, since $\sigma = \gamma$. For solids, the average electrostrictive term ($\Delta\epsilon/\Delta E$) can be experimentally estimated, and as previously argued by Couchman and Davidson,[39] is found to be a second-order effect which can be neglected. Therefore for practical purposes, both liquid and solid electrodes obey the same Lippmann equation ($\partial\gamma/\partial E|_{T,\mu_k} = -q$). Hence the surface energy (γ) can be obtained in the same way as for liquid Hg electrodes by measuring the variation of charge (q) with potential (E) at constant composition of the solution.[16]

In the case of constant interfacial capacitance, C, the surface energy (γ) should then be equal to $q^2/2C$ or $CE^2/2$. The surface energy γ is therefore quadratic in q or E, and the electrocapillary curve is parabolic with a maximum at the potential of zero charge (PZC). In contrast, the surface stress, σ, need not have an extremum at the PZC. Detailed discussions on the thermodynamics of solid electrodes are reviewed in references.[16,21,40]

RESULTS AND DISCUSSION

Morphology of the Gold Sensing Surface. A cyclic voltammogram (CV) in 0.1 M $HClO_4$ of an Au(111)-textured microcantilever WE is presented in Figure 1, with an inset showing the charge density change as a function of potential of the gold electrode in the electrical double layer region. An SEM image of the WE gold surface is shown in Figure 3A. The potential of zero charge was determined to be +285 mV vs Ag/AgCl (immersed in 3 M NaCl) using chronocoulometric measurements published by Lipkowski et al.[41]

We have estimated the surface energy change in the double layer region by integrating the charge density with respect to the potential using eq 3. Figure 2 shows the variation of the surface energy calculated[42] from the Lippmann equation as a function of potential. The surface energy change versus potential (electrocapillary curve) has by definition a maximum at the PZC. The surface energy change measured over the potential range investigated (−0.065 N/m) is close to that on a single-crystal Au(111) electrode.[44] The surface energy curves exhibit a parabolic dependence with potential and charge. With an assumption of a constant capacitance of the interface, C, the surface energy (γ) curve can be well fitted to an equation of the form $\gamma = C/2(E - E_{PZC})^2$. A value, in 0.1 M $HClO_4$, for the capacitance of the double layer of

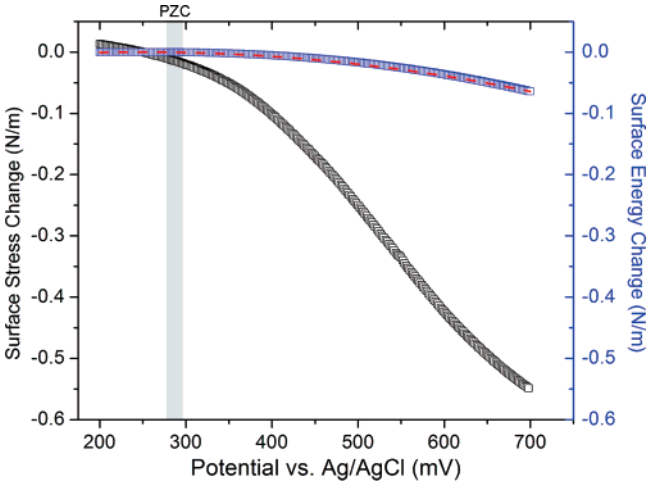

Figure 2. Surface stress change as function of electrode potential for the Au(111)-textured microcantilever in 0.1 M $HClO_4$ electrolyte solution (black line). The surface energy change (blue line) along with a parabolic fit (red dashed). The data was cut below +200 mV to prevent superfluous charge from hydrogen evolution from being included in the evaluation.

70 ± 10 μF cm^{-2} is found from the fit. This is in reasonable agreement with previously reported values[43] and to a first order matches the slope of the inset in Figure 1. The results, presented in Figures 1 and 2, reveal that electrochemical data obtained using a microcantilever WE are characteristic of polycrystalline Au(111)-textured films and are consistent with macroscopic electrodes results.[44]

In contrast to the surface energy change, the surface stress measured as a function of applied potential does not exhibit a parabolic shape (Figure 2). The surface stress change measured over the same potential window is -0.55 ± 0.06 N/m for a set of 20 independent experiments. This surface stress change is therefore 10-fold larger than the surface energy change for the polycrystalline Au(111)-textured microcantilever surface in 0.1 M $HClO_4$. The potential dependent surface stress profile in Figure 2 for a polycrystalline Au(111)-textured microcantilever (Figure 3A) is in excellent agreement with previous results by Ibach et al.[23,45−47] obtained on single-crystal Au(111) electrodes. For the particular case of perchlorate adsorption, using a polycrystalline Au(111)-textured surface (shown in Figure 3A), one can therefore reproduce the data acquired employing atomically flat single-crystal macroscopic electrode surfaces.[47] This suggests that parameters such as grain size, film roughness, or grain boundaries may not strongly influence the induced surface stress for anion adsorption at the solid−liquid interface.

Surfaces with different morphologies were used to assess the role played by grain boundaries, grain sizes, and discontinuities

(39) Couchman, P. R.; Davidson, C. R. *J. Electroanal. Chem.* **1977**, *85*, 407−409.
(40) Valincius, G. *J. Electroanal. Chem.* **1999**, *478*, 40−49.
(41) Lipkowski, J.; Shi, Z.; Chen, A.; Pettinger, B.; Bilger, Ch. *Electrochim. Acta* **1998**, *44*, 1037−1052.
(42) The uncertainties associated with the surface area of the WE and with the magnitude of the current (due to an unavoidable presence of oxygen in the electrolyte) produce an error on the evaluation of the surface energy which is difficult to quantify. Nevertheless, it is informative to look at the magnitude of the surface energy change as well as its dependence on the applied potential to gain a better understanding of the different contributions of each term of the Shuttleworth equation.
(43) Shi, Z.; Lipkowski, J. *J. Electroanal. Chem.* **1996**, *403*, 225−239.
(44) Vasiljevic, N.; Trimble, T.; Dimitrov, N.; Sieradzki, K. *Langmuir* **2004**, *20*, 6639−6643.
(45) Including a correction factor of 0.8260 which was later calculated using finite element analysis, ref 46, because of the particular geometry of the clamped beam used.
(46) Dahmen, K.; Lehwald, S.; Ibach, H. *Surf. Sci.* **2000**, *446*, 161−173.
(47) The cantilever in these experiments has a rectangular shape of 6 mm × 3 mm clamped at one end. In order to ensure that changes in the surface stress would occur only on one side, the lower face of the sample was covered with nail polish. The change in the vertical position of the sample is measured by the STM tip. Prior to the measurements, the Au single crystals were annealed at 800 °C for 2 h in an oxygen atmosphere and for 1 h in an argon atmosphere. Afterwards, the crystals were allowed to cool in an argon atmosphere.

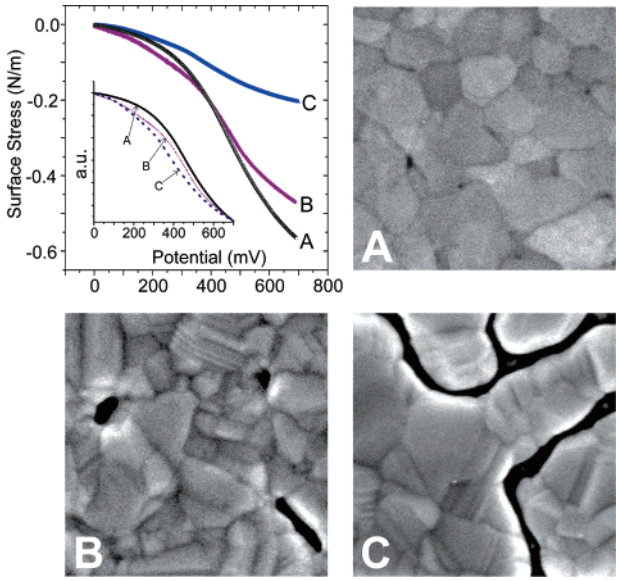

Figure 3. Potential-induced surface stress response of the various gold surface morphologies shown in the bordering SEM images. The inset of the graph represents data from surface A (—) and, surface B and C normalized by a constant factor (•••• and ----, respectively). Surface A: evaporated gold film on a Ti adhesion layer, image size 500 × 500 nm^2. Surface B: sputtered gold film at 300 °C grown on a Nb adhesion layer, image size 500 × 500 nm^2. Surface C: sputtered gold film at 400 °C grown on a Nb adhesion layer, image size 500 × 500 nm^2.

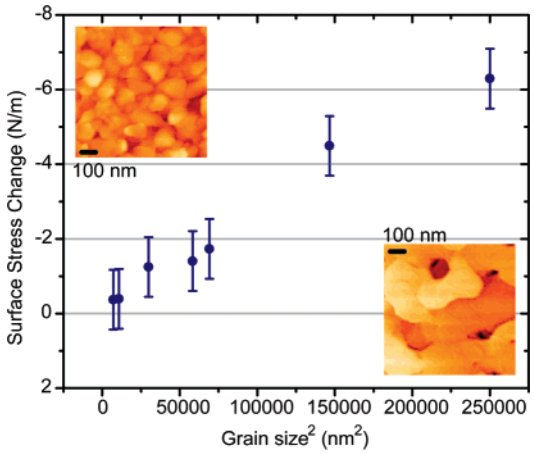

Figure 4. The surface stress induced by octanethiol SAM formation as a function of the square of the gold substrate grain size. The standard deviations of the grain sizes are not shown. Inset are scanning tunneling microscopy images of the smaller-grained (top left) and larger-grained (bottom right) gold surfaces, deposited at different temperatures on silicon nitride cantilevers without an adhesion layer.

in determining the measured surface stress. Three different surfaces are shown in Figure 3. The surface in Figure 3A has a grain size of 100 ± 60 nm, with flat and connected grains. This surface possesses no apparent discontinuities. The surface in Figure 3B has a much wider distribution of grain sizes. The grains remain flat, but the surface contains several voids between the grains. Overall the gold film is continuous. This is in contrast with the surface in Figure 3C, where the gold film is discontinuous and composed of isolated flat islands.

Each of the gold films was subjected to a potential scan from 0 to +700 mV, in 0.1 M $HClO_4$, while recording the induced surface stress. The results are shown in Figure 3. The inset of the graph shows the surface stress change for surface A, together with surfaces B and C which were normalized using a scaling factor (Figure 3). The surface stress response of the evaporated (A) and sputtered (B,C) gold films are qualitatively similar. The smaller surface stress value generated on the sputtered films is most probably caused by the presence of voids and channels between the grains. The discontinuities between the grains likely prevent the strain from propagating along the entire surface so that some stress is lost at the boundaries between discontinuous islands. However, the different grain size distributions do not have a dramatic impact on the surface stress response (see inset of the graph of Figure 3). The polycrystalline electrodes with surfaces B and C in Figure 3 may also possess some small domains with different crystal faces and edges presented to the electrolyte which exhibit different properties (e.g., PZC or work function) as well as a different capacitance (i.e., carry different charge). Hence, we propose that the negative shift in the surface stress-potential curves of surfaces B and C observed in the inset is a consequence of a different PZC value. Unfortunately, the impact of the wider grain size distribution of surface B compared to A remains a point of discussion, given that the difference between the surface stress curves of the two surfaces is close to the accuracy of the measurement.[31] Nevertheless, its effect on the induced surface stress is estimated to be ≤10%. The SEM image of surface C shows increased discontinuities in the film compared to surfaces A and B. This suggests that the magnitude of the surface stress is mostly affected by the presence of voids and channels between the grains. Discontinuities in the gold surface prevent the generated surface stress from being efficiently transferred to the Si beam.

In the case of the potential-induced anion adsorption, the surface stress response is more dependent on the continuity of the gold sensing surface than on its average grain size. Indeed, as discussed above, the surface stress change measured on surface A is in excellent agreement with previously reported values by Ibach et al.[23,46] on single-crystal Au(111) surfaces and is quantitatively reproducible. However, this observation cannot be generalized. In the following, we investigate a different model system: the vapor phase alkanethiol adsorption on gold.

We have observed that the surface stress induced by the gas-phase formation of alkanethiol SAMs on gold surfaces is strongly dependent on the substrate morphology. SAM formed on small-grained gold induce a smaller change in surface stress than for monolayers formed on larger grains.[26,32] The domain size and the conformation of adsorbed thiol molecules are strongly correlated with the grain size of the underlying gold surface. In fact, alkanethiol SAM on small gold grains can remain kinetically trapped in an intermediate lying-down (striped) phase, while SAM formation on larger grains results in the more familiar standing-up phase which produces a larger surface stress.[26,32]

These effects were further investigated by studying the gas phase adsorption of octanethiol on gold surfaces as a model system. Figure 4 presents the surface stress induced by octanethiol SAM formation as a function of the average gold grain area. Remarkably, the induced change in surface stress increases by as much as 25-fold with increasing gold grain size area. These

results suggest that the surface stresses measured in previous reports[1,48,49] for alkanethiol SAM formation from the vapor phase were for incomplete monolayers in the lying-down phase formed on small-grained gold. However, as shown in Figure 4, the surface stress is strongly dependent upon the average gold surface grain area in part because the thiol adsorption isotherm is strongly grain size dependent.[26] Because of the large variability of grain sizes for a given sample (e.g., 500 ± 400 nm for the largest grain size shown), a coexistence of the kinetically hindered lying-down phase (formed on small gold grains) and the standing-up phase (formed on large gold grains) is expected. While the results of Figure 4 suggests that a higher proportion of the SAM is in the standing-up phase when formed on large-grained gold, the gold grain size threshold value at which the SAM is no longer kinetically trapped and able to undergo the transition to the standing-up phase is not discernible.

The maximum theoretical change in surface stress induced by the formation of an alkanethiol SAM on gold remains to be determined. The data in Figure 4 do not yield the maximum value but suggest that the surface stress can be in excess of −7 N/m for a complete, defect-free octanethiol SAM. Since the critical gold grain size at which the transition into the standing-up phase occurs is not known, it is difficult to extrapolate what this maximum theoretical surface stress value might be. Nevertheless, to obtain reliable and reproducible results with microcantilever-based surface stress sensors decorated with an alkanethiol SAM formed in the gas phase, it is important to control the gold surface morphology.

Reliable surface stress measurements require that the surface stress be completely transferred to the underlying substrate. This condition is fulfilled for results obtained on single crystal cantilevers and on surfaces with thin evaporated films deposited on an adhesion layer (i.e., Figure 2). In addition, the results of Figure 4 demonstrate that large surface stress changes can be observed on a film without an explicit adhesion layer. Nonetheless, we subjected a gold film which had been deposited directly on a silicon microcantilever (i.e., without an adhesion layer) to a potential scan from 0 to +700 mV, in 0.1 M $HClO_4$. The adhesion was not quantitatively assessed, but the film can be easily scratched or peeled off the surface. Care was taken when immersing this gold-coated microcantilever without an adhesion layer into the electrolyte solution to prevent the surface tension of the liquid from stripping off the film. A monotonic change in surface stress was observed, equivalent to the one observed when an adhesion layer is present. The potential-induced surface stress curve, of the gold film without an adhesion layer, reveals that the magnitude of the surface stress change is not affected by the poor adhesion (data not shown). The adhesion of the metal film must therefore be exceptionally poor to not properly transfer the surface stress to the underlying substrate.

Cleanliness of the Gold Sensing Surface. Freshly evaporated gold surfaces exposed to thiols minutes after evaporation were used for the alkanethiol experiments, and all of the potential-induced surface stress measurements obtained on gold-coated microcantilevers were performed on electrochemically cleaned surfaces.

The role played by ambient adsorbate contamination was measured by simply exposing a freshly evaporated gold film to the lab environment for one week. X-ray photoelectron spectroscopy (XPS) performed on gold surfaces thus prepared revealed the presence of contamination species containing carbon and oxygen. The effect of surface contaminants for the case of alkanethiol adsorption from the vapor phase was previously reported.[26] To determine the effect of surface contamination for the case of anion adsorption at the solid−liquid interface, a contaminated gold-coated microcantilever was placed in the electrochemical cell as the WE and the potential was scanned from 0 to +700 mV while recording the potential-induced surface stress. The surface was then electrochemically cleaned by cycling the potential between 0 and +1500 mV. The surface is cleaned through oxidation/reduction of the gold which removes surface contaminants. A second surface stress response for the newly cleaned gold surface was then measured in the potential region between 0 and +700 mV.

The surface stress response for the clean and contaminated gold-coated microcantilever in 0.1 M $HClO_4$ is shown in Figure 5a as a function of the electrode potential. The form and magnitude of the potential-induced surface stress profile of the contaminated surface is quite different to that obtained for the clean gold surface. Not only is the magnitude smaller for the *unclean* surface but the shape of the profile is different. Unlike the clean surface, the surface stress versus potential curve for the contaminated gold yields a parabolic relationship. This parabolic behavior is reminiscent of the change in surface energy and the resemblance between Figures 2 and Figure 5a is striking. However, at constant interfacial capacitance (i.e, $q = C/E$), the Lippmann equation predicts that the surface *energy* and not the surface stress of a solid surface should be parabolic with potential. Superficially, this observation is puzzling and could be misinterpreted[9−11,14] as evidence that for solid electrodes, surfaces stress is equivalent to surface energy (as is the case for liquid electrodes). Figure 5a reveals that ambient adsorbates on the gold sensing surface both qualitatively and quantitatively alter the potential-induced surface stress response. It is therefore essential to employ freshly evaporated and/or electrochemically cleaned surfaces if meaningful results are to be obtained.

In trying to understand the shape of the surface stress versus potential profile, it is useful to plot the surface stress versus surface charge density (Figure 5b). The change in the surface stress for a clean gold microcantilever is linearly dependent on the surface charge. The data were fitted to a straight line over the range of 5 to 25 μC cm^{-2} and a slope of ca. −2 V was obtained. A linear dependence on Au(111) was first reported by Haiss and Sass[19] who measured a slope of −0.91 V on flame annealed gold-coated glass cantilevers. This was later confirmed by Ibach[50] on single-crystal gold cantilevers. The difference between these charge-induced surface stress values may be attributed to differences in the measured value of the interfacial capacitance or inconsistencies in the quantitation of the surface stress by various methods.[23,46] Recall that the interfacial capacitance found herein of ∼70 μF cm^{-2} agrees with the values reported by Lipkowski et al.,[43] and that the surface stress change measured is in excellent agreement with previously reported value by Ibach et al.[23,46] Moreover, a recent ab initio study of surface stress response to charging calculated a slope of −1.86 V for a Au (111) surface.[51] Integration of the relevant CV for the contaminated electrode surface also yields a linear dependence of surface stress on surface charge density (Figure 5b).

(48) Berger, R.; Delamarche, E.; Lang, H. P.; Gerber, Ch.; Gimzewski, J. K.; Meyer, E.; Guntherodt, H.-J. *Appl. Phys. A* **1998**, *66*, S55.
(49) Hansen, A. G.; Mortensen, M. W.; Andersen, J. E. T.; Ulstrup, J.; Kuhle, A.; Garnaes, J.; Boisen, A. *Probe Microsc.* **2001**, *2*, 139.
(50) Ibach, H. *Electrochim. Acta* **1999**, *45*, 575−581.

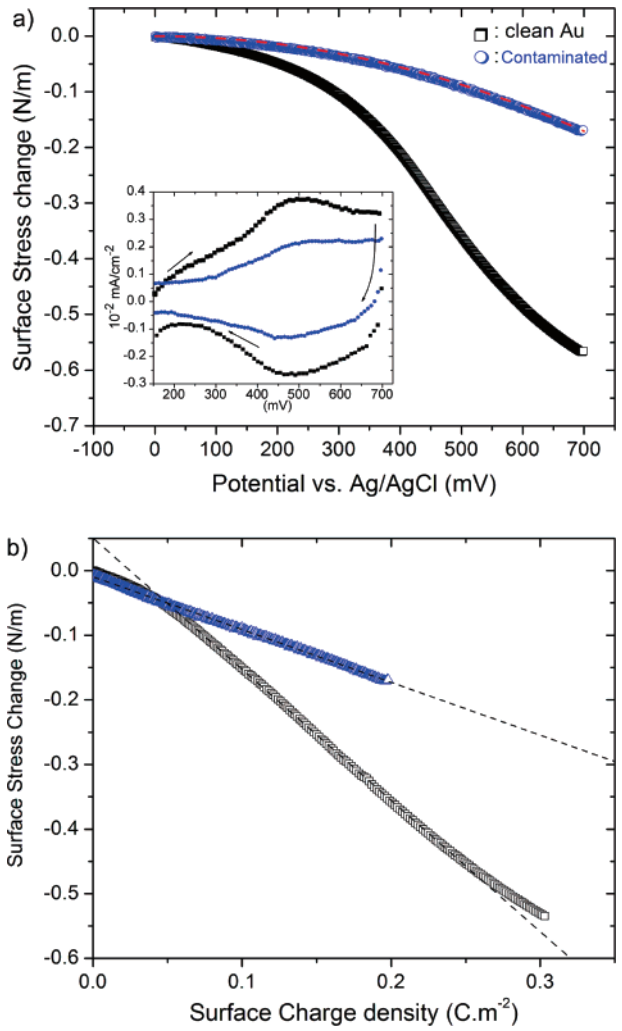

Figure 5. (a) Potential-induced surface stress in 0.1 M $HClO_4$. Surface stress response of a freshly cleaned gold surface (black squares). Surface stress of a contaminated gold surface (blue circles) with a parabolic fit (red dash). The inset is the corresponding CV for both clean gold (black squares) and contaminated gold (blue circles, lower current values) surfaces. The surface stress results correspond to the anodic sweep (positive direction). (b) Surface stress versus surface charge density for both clean (black square) and contaminated (blue triangle) gold-coated cantilevers. Data represent a potential scan from +235 to +700 mV. The deviation from linearity observed on the clean gold at both low and high surface charge density is attributed to the presence of superfluous charge (hydrogen evolution and oxide formation, respectively) included in the evaluation of the electrode surface charge density.

This linear relationship between charge and surface stress for a Au(111) surface enables one to predict the potential-induced surface stress profile from the cyclic voltammogram itself. We use this experimentally determined relationship as a starting point in the following analysis, where

$$d\sigma = k dq \tag{4}$$

and k is a constant (i.e., the slopes in Figure 5b). The charge on the electrode is a function of both the potential, E, and the fractional coverage of specifically adsorbing species, θ, and can be expressed as a full differential.

$$dq = \left(\frac{\partial q}{\partial \theta}\right)_E d\theta + \left(\frac{\partial q}{\partial E}\right)_\theta dE \tag{5}$$

which can be substituted into eq 4. Dividing by dE then provides

$$\frac{d\sigma}{dE} = k\left[\left(\frac{\partial q}{\partial \theta}\right)_E \frac{d\theta}{dE} + \left(\frac{\partial q}{\partial E}\right)_\theta\right] \tag{6}$$

The first term on the right-hand side is commonly referred to as the pseudo capacitance whereas the second term is denoted the true capacitance. Rearrangement of eq 6 provides

$$d\sigma = k(C_{pseudo} + C_{true})dE \tag{7}$$

Experimentally, one measures the total capacitance C which is the sum of C_{pseudo} and C_{true}. In general, the value of the measured capacitance is potential dependent and the relationship between surface stress and potential is determined by the integral of eq 7. Given that $C \propto vI$ where v is the voltammetric sweep rate and I is the current, the capacitances of the two systems studied (clean and contaminated gold) can be estimated from the cyclic voltammograms shown in the inset of Figure 5a. The CVs clearly demonstrate that in both cases the capacitance varies with potential. However, the magnitude of the currents is greater for the *clean* gold surface CV, especially in the potential region where perchlorate ions adsorb on the gold surface (i.e., the peak at ~500 mV). We believe that this correspondingly higher capacitance and greater dependence of the capacitance on the electrode potential is responsible for the differences in the curvature of the potential-induced surface stress. We have thus rationalized the observed differences in Figure 5a by demonstrating that the surface stress response of a system with a linear surface stress−charge relationship is dictated by the capacitance of the interface.

CONCLUSION

The role played by the state of the gold sensing surface on the microcantilever surface stress response was examined. The surface morphology was found to strongly influence the surface stress response for molecular adsorption where ordering of the molecules is dependent on their coverage and domain size. The results from the vapor phase alkanethiol adsorption on gold demonstrate that the induced surface stress is highly dependent on the sensing surface average grain size. In contrast, for adsorption of anions, the surface stress on smooth and continuous polycrystalline Au(111)-textured films are in an excellent agreement with other Au(111) single-crystal results. For both model systems studied, discontinuities in the gold surface significantly affect the magnitude of the induced surface stress irrespective of the adsorbate. While the gold grain size does not affect perchlorate adsorption, it does affect the final structure of a SAM and thus has a strong influence on the magnitude of the induced surface stress.

The adhesion of the gold films was found to be adequate in completely transferring the surface stress to the underlying substrate even in the absence of an adhesion promoting layer such as Ti, Cr, or Nb. Contrary to an earlier report,[52] during anion adsorption on gold there is no evidence of a parabolic shape of the surface stress-potential curve for the types of clean evaporated

(51) Umeno, Y.; Elsasser, C.; Meyer, B.; Gumbsch, P.; Nothacker, N.; Weissmuller, J.; Evers, F. *Europhys. Lett.* **2007**, 78, 13001.

(52) See ref 22, pages 633 to 634.

and sputtered films studied. The cleanliness of the gold sensing surface does however influence the surface stress-response both quantitatively and qualitatively at the solid−liquid and at the solid−gas interface.[26] In the particular case where a gold surface is contaminated with adsorbates, the surface stress-potential response may qualitatively resembles the surface energy-potential response calculated from the Lippmann equation, misleading to the conclusion that surface stress is dominated by surface energy change.

ACKNOWLEDGMENT

This work was supported by the Natural Sciences and Engineering Research Council of Canada (NSERC) and Canadian Institute of Health Research (CIHR). V.T.-C. and M.G. acknowledge the financial support given by McGill University through its McGill Major Fellowships program. M.G. would like to thank Le Fonds Québécois de la Recherche sur la Nature et les Technologies (FQRNT) for financial support (Doctoral Fellowship). I.J.B. would like to thank both NSERC and the Tomlinson Foundation of McGill for postdoctoral funding. The authors thank L. Y. Beaulieu, H. Bourque and P. J. Williams for many helpful discussions, E. Del Campo for machining the instruments, and R. Gagnon for technical assistance. V.T.-C. and M.G. contributed equally to this work.

Received for review June 12, 2007. Accepted August 17, 2007.

AC071243D